ELSEVIER

Physica D 111 (1998) 16–26

PHYSICA D

Some global properties of a pair of coupled maps: Quasi-symmetry, periodicity, and synchronicity

F.E. Udwadia [a,*], N. Raju [b,1]

[a] *Department of Mechanical Engineering, 430K Olin Hall, University of Southern California, Los Angeles, CA 90089-1453, USA*

[b] *Department of Mechanical Engineering, University of Southern California, Los Angeles, CA 90089-1453, USA*

Received 20 February 1997; received in revised form 20 May 1997; accepted 2 June 1997
Communicated by Y. Kuramoto

Abstract

We analyze some global, generic properties of a pair of coupled maps. These generic properties are then utilized to investigate how the extent of coupling affects the behavior of the coupled system. Quasi-symmtery of the global behavior is discussed. Numerical validation of the analytical results is provided.

1. Introduction

Nonlinear maps have extensively been used to model several nonlinear dynamical systems especially because usually only discrete measurements are possible and from these discrete data one needs to reconstruct the dynamics. Discrete systems are used in a large number of scientific disciplines ranging from fluid dynamics to ecological modeling. For instance, Ricker [13], based on empirical evidence, has postulated that the population dynamics of a prey species can be modeled using exponential maps if the predator species captures the prey species in random encounters. The use of logistic maps to simulate population growth is also well-known [2,10].

A typical example of a discrete time system is a one-dimensional map

$$x_{n+1} = f(x_n). \tag{1}$$

If an initial condition x_0 is specified at time level $n = 0$, the system state at time level $n = 1$ is $x_1 = f(x_0)$, and so on. The function f can be any linear or nonlinear map, for instance, the exponential map, $f(x) = x\exp(r(1-x))$, as per Ricker [13], to model the population dynamics of a prey species.

A two-dimensional discrete-time system can be obtained by coupling two such one-dimensional maps, say

$$\begin{aligned} x_{n+1} &= df(x_n) + (1-d)f(y_n), \\ y_{n+1} &= (1-d)f(x_n) + df(y_n), \end{aligned} \tag{2}$$

where d is the coupling parameter. This form of coupling often arises in physical systems and has been used by several researchers in the past. See, for example, [6]. One can think of $f(x_n)$ and $f(y_n)$ as simulating the population dynamics of a particular species (the species can be any biological or chemical species,

* Corresponding author.
[1] Present address: UMEVoice, Novato, CA, USA.

PII S0167-2789(97)00134-6

or even scalar fields such as temperature) at two adjacent locations. If, after every time increment, only a fraction d of these species remains in the same location and the rest migrate to the other location, their dynamics is described by Eq. (2). The coupling parameter d can vary between zero and unity. If $d = 1$, there is no coupling and if $d < 1$, there is coupling. We shall denote the mapping described by Eq. (2), for brevity, as

$$(x_{n+1}, y_{n+1}) = M(d) \circ (x_n, y_n), \tag{3}$$

to explicitly indicate the dependence on the parameter d. In Section 2 we present some analytical results related to the global behavior of such coupled maps. Additional universal dynamics is outlined through numerical investigations in Section 3. The significance of these results is discussed in Section 4.

2. Analytical results

Result 1. For each orbit $\{(\hat{x}_n, \hat{y}_n) \mid n = 0, 1, 2, \ldots\}$, corresponding to the parameter value d, there corresponds an orbit $\{(\hat{y}_n, \hat{x}_n) \mid n = 0, 1, 2, \ldots\}$.

Proof. This result is obvious from Eq. (2) since the interchanges

$$\left\{ \begin{array}{l} x_n \to y_n \\ y_n \to x_n \end{array} \right\} \Longrightarrow \left\{ \begin{array}{l} x_{n+1} \to y_{n+1} \\ y_{n+1} \to x_{n+1} \end{array} \right\}. \qquad \square$$

Corollary 1. For each n-periodic orbit of the map (2) described by $\{(\hat{x}_n, \hat{y}_n) \mid n = 0, 1, 2, \ldots\}$ corresponding to the parameter d, there exists another n-periodic orbit described by $\{(\hat{y}_n, \hat{x}_n) \mid n = 0, 1, 2, \ldots\}$.

Proof. The result is a special case of Result 1 when the orbits are periodic. $\square$

Result 2. Consider the orbit $\{(\hat{x}_n, \hat{y}_n) \mid n = 0, 1, 2, \ldots\}$ corresponding to a certain value of the parameter $d = \frac{1}{2} - d_0$, $0 \le d_0 \le \frac{1}{2}$. For each such orbit, there corresponds an orbit given by $\{(\hat{x}_0, \hat{y}_0), (\hat{y}_1, \hat{x}_1), (\hat{x}_2, \hat{y}_2), (\hat{y}_3, \hat{x}_3), \ldots\}$, corresponding to the parameter $d = \frac{1}{2} + d_0$, i.e., each alternate point of the second orbit has its x- and y-coordinate switched with respect to the corresponding point of the first orbit.

Proof. The result follows from the observation that for an initial point $(\hat{x}_n, \hat{y}_n)$, if

$$(\hat{x}_{n+1}, \hat{y}_{n+1}) = M(\tfrac{1}{2} - d_0) \circ (\hat{x}_n, \hat{y}_n), \tag{4}$$

then,

$$\begin{aligned} (\tilde{x}_{n+1}, \tilde{y}_{n+1}) &= M(\tfrac{1}{2} + d_0) \circ (\hat{x}_n, \hat{y}_n) \\ &= (\hat{y}_{n+1}, \hat{x}_{n+1}). \end{aligned} \tag{5}$$

Furthermore denoting,

$$(\hat{x}_{n+2}, \hat{y}_{n+2}) = M(\tfrac{1}{2} - d_0) \circ (\hat{x}_{n+1}, \hat{y}_{n+1}), \tag{6}$$

we find that

$$\begin{aligned} (\tilde{x}_{n+2}, \tilde{y}_{n+2}) &= M(\tfrac{1}{2} + d_0) \circ (\tilde{x}_{n+1}, \tilde{y}_{n+1}) \\ &= (\hat{x}_{n+2}, \hat{y}_{n+2}), \end{aligned} \tag{7}$$

and hence the result. $\square$

Corollary 2. If the map $M(\frac{1}{2} - d_0)$, $0 \le d_0 \le \frac{1}{2}$, has a $2n$-period orbit starting from some (x_0, y_0), $n = 1, 2, \ldots$, then the map $M(\frac{1}{2} + d_0)$ must have a $2n$-period orbit starting from the same point (x_0, y_0), $n = 1, 2, \ldots$

Proof. This again is obvious from Result 2. $\square$

Corollary 3. If the map $M(\frac{1}{2} - d_0)$, $0 \le d_0 \le \frac{1}{2}$, has a $(2n - 1)$-period orbit starting some (x_0, y_0), $n = 1, 2, \ldots$, with $x_0 \ne y_0$, then the map $M(\frac{1}{2} + d_0)$ must have a $2(2n - 1)$-period starting from the same point (x_0, y_0), $n = 1, 2, \ldots$

Proof. This again is obvious from Result 2. $\square$

Result 3. The orbit of the map (2) starting with (x_0, x_0) will always consist of points of the form (x_n, x_n). In other words, orbits which begin on the diagonal in the (x, y) phase space lie entirely on the diagonal.

Proof. This follows from the observation that

$$M(d) \circ (x_{n+1}, x_{n+1}) = M(d) \circ (x_n, x_n). \qquad \square \tag{8}$$

The above result indicates that for orbits that begin on the diagonal in the phase space, each state of the dynamical system behaves as if it were governed by one-dimensional map of the form of Eq. (1).

Result 4. For $d = \frac{1}{2}$ the orbit of the map (2) starting with (x_0, y_0) will consist of points of the form (x_n, x_n) after the first iteration.

Proof. This result is obvious from the observation that the map (2) redistributes the sum of $f(x_n)$ and $f(y_n)$ equally after every iteration. □

Result 5. Each Lyapunov exponent of the map $M(\frac{1}{2} - d_0)$, $0 \leq d_0 \leq \frac{1}{2}$, starting from some (x_0, y_0) is the same as that of the map $M(\frac{1}{2} + d_0)$ starting from the same point (x_0, y_0).

Proof. Let

$$M(\tfrac{1}{2} - d_0) \circ (x_n, y_n) = (x_{n+1}, y_{n+1}). \tag{9}$$

Let us further denote

$$M(\tfrac{1}{2} + d_0) \circ (x_n, y_n) = (\tilde{x}_{n+1}, \tilde{y}_{n+1}). \tag{10}$$

By Result 2,

$$(\tilde{x}_{n+1}, \tilde{y}_{n+1}) = (y_{n+1}, x_{n+1}) \tag{11}$$

and

$$\begin{aligned} &M(\tfrac{1}{2} - d_0) \circ (x_{n+1}, y_{n+1}) \\ &\quad = M(\tfrac{1}{2} + d_0) \circ (\tilde{x}_{n+1}, \tilde{y}_{n+1}) \\ &\quad = (x_{n+2}, y_{n+2}). \end{aligned} \tag{12}$$

The Lyapunov exponents are given by

$$\lambda_i = \lim_{n\to\infty} \frac{\log_e[|\mu_i|]}{n}. \tag{13}$$

where μ_i are the eigenvalues of the product of the Jacobian matrices at every iteration. Being a two-dimensional system, Eq. (2) has two Lyapunov exponents. The Jacobian matrix for this system is

$$\begin{aligned} &J_n\,[M(d)]_{(x_n,y_n)} \\ &\quad = \begin{bmatrix} df'(x_n) & (1-d)f'(y_n) \\ (1-d)f'(x_n) & df'(y_n) \end{bmatrix}. \end{aligned} \tag{14}$$

Therefore, the Jacobian of the map $M(\frac{1}{2} - d_0)$ starting from (x_n, y_n) is of the form

$$J_n[M(\tfrac{1}{2} - d_0)]_{(x_n,y_n)} = \begin{bmatrix} a_{11} & a_{12} \\ a_{21} & a_{22} \end{bmatrix}. \tag{15}$$

Also the Jacobian of the map $M(\frac{1}{2} + d_0)$ starting from the same point $(x_n, y_n) = (\tilde{x}_n, \tilde{y}_n)$ is of the form

$$\begin{aligned} \tilde{J}_n[M(\tfrac{1}{2} + d_0)]_{(\tilde{x}_n,\tilde{y}_n)} &= \tilde{J}_n[M(\tfrac{1}{2} + d_0)]_{(x_n,y_n)} \\ &= \begin{bmatrix} a_{21} & a_{22} \\ a_{11} & a_{12} \end{bmatrix}. \end{aligned} \tag{16}$$

Similarly,

$$J_{n+1}[M(\tfrac{1}{2} - d_0)]_{(x_{n+1},y_{n+1})} = \begin{bmatrix} b_{11} & b_{12} \\ b_{21} & b_{22} \end{bmatrix}. \tag{17}$$

$$\begin{aligned} &\tilde{J}_{n+1}[M(\tfrac{1}{2} + d_0)]_{(\tilde{x}_{n+1},\tilde{y}_{n+1})} \\ &\quad = \tilde{J}_{n+1}[M(\tfrac{1}{2} + d_0)]_{(y_{n+1},x_{n+1})} \\ &\quad = \begin{bmatrix} b_{12} & b_{11} \\ b_{22} & b_{21} \end{bmatrix}. \end{aligned} \tag{18}$$

Hence, it is seen that

$$J_{n+1} J_n = \tilde{J}_{n+1} \tilde{J}_n. \tag{19}$$

Therefore the eigenvalues and the Lyapunov exponents are symmetric about $d = \frac{1}{2}$. □

Result 6. When $d = \frac{1}{2}$, one Lyapunov exponent tends to $-\infty$.

Proof. On setting $d = \frac{1}{2}$ in Eq. (14) the determinant vanishes and hence the result. □

Notice that the above results are independent of the functional form of the map f. Thus, these results are applicable to any general map f coupled in the manner described earlier.

Result 3 has several implications. Suppose that x_n is a fixed point of the one-dimensional map $x_{n+1} = f(x_n)$, then the point (x_n, x_n) is a fixed point of the two-dimensional system (2) for all values of the coupling parameter d. Further, the fixed point (x_n, x_n) of the two-dimensional system has the same stability characteristics as the fixed point x_n of the one-dimensional system.

Similarly, if the one-dimensional map $x_{n+1} = f(x_n)$ has a periodic orbit $x_i | i = 1, 2, \ldots, N$, then the system (2) also has a periodic orbit of the form $(x_i, x_i) | i = 1, 2, \ldots, N$. The stability characteristics of both these orbits are furthermore identical. Thus by coupling two nonlinear maps, the same periodic behavior observed in the one-dimensional map can be reproduced for *all* values of d.

3. Numerical results

In addition, for certain values d other fixed points and periodic trajectories arise. Such additional periodic behavior has been observed by us in numerical simulations of coupled logistic maps and coupled exponential maps [16]. Let us consider the exponential map such that $f(x_n)$ in Eq. (2) is expressed by $x_n \exp(r(1 - x_n))$. If we choose r so that the one-dimensional map $x_{n+1} = x_n \exp(r(1 - x_n))$, exhibits chaotic trajectories, then by coupling two such maps in the manner described by Eq. (2), periodic behavior can be obtained as demonstrated in Fig. 1. Similar periodic behavior is demonstrated in the Lyapunov exponent plot (Fig. 6) in which for certain ranges of d both the exponents are negative. Thus coupling two chaotic systems can stabilize both of them. In fact, as Fig. 1 shows, for $0.03 \lesssim d \lesssim 0.13$ we observe two one-period orbits, i.e., by coupling two chaotic units we can arrive at complete equilibrium (Fig. 1). This stabilizing phenomenon may very well explain why there is so much stability in this physical world despite all the reported chaos.

Apart from stabilizing nonlinear systems, coupling can synchronize nonlinear systems, i.e., coupling can force the two subunits to behave identically. Such synchronization may have several applications. For instance, the use of chaotic synchronization in communication systems has been investigated by several authors say [3,11]. There, an informational signal is modulated on a chaotic signal and then transmitted. Yet, the synchronization dealt with in this paper differs from these investigations in that there is no "driving" system or "driven" system, and the flow of information is bidirectional (see Eq. (2)). Other applications may arise in neuro-biological systems. Recent studies indicate synchronized neural activity in the visual cortex of cats [4] and monkeys [8,9].

Typically, the chaotic response of the nonlinear system (2) for an initial condition not on the diagonal ($x_0 \neq y_0$) is over a region of the xy-plane. (If the initial condition is on the diagonal, the response remains on the diagonal as per Result 4). But when synchronization is observed, the response of the coupled system, after a large number of iterations, is limited to the line $x = y$. Thus, instead of spanning the two-dimensional surface, the dynamics is confined to a one-dimensional line. This one-dimensional dynamics may be viewed as a step towards stabilization because, if the dimension further drops to zero, then periodic behavior results.

When the two units evolve synchronously, both populations are identical, i.e., $x = y$. Therefore, the difference between the two populations $x - y$ should be identically zero. To understand how this synchronicity varies with the coupling parameter d, we plot the difference, $x - y$ in Fig. 2(c). It can be seen that the range of d for which the dynamics is synchronous is significant.

Synchronized motion of a similar nature has been treated in [5,12,14,18]. Fujisaka and Yamada [5] outlined a general stability theory of synchronized motion for nonlinear systems. They [5] were the first to discuss the possibility of the experimental observation of the largest Lyapunov exponent of a chaotic system, see also [14].

We note that besides the zone of synchronized behavior, the coupled exponential map displays a variety of behavior over the range of d values of interest. The overall dynamics of the coupled exponential map system can broadly be divided into seven zones as in Fig. 2(c). The transition from one zone to another is marked by a bifurcation with respect to the parameter d. Either a tangent bifurcation or a Hopf-like bifurcation may mark the transition from one zone to another, for details see [16]. It should be pointed out that numerical simulations show that the seven-zone dynamics described hereunder does not seem to be displayed by coupled maps each of which have non-negative Schwartzian curvature, for instance piecewise

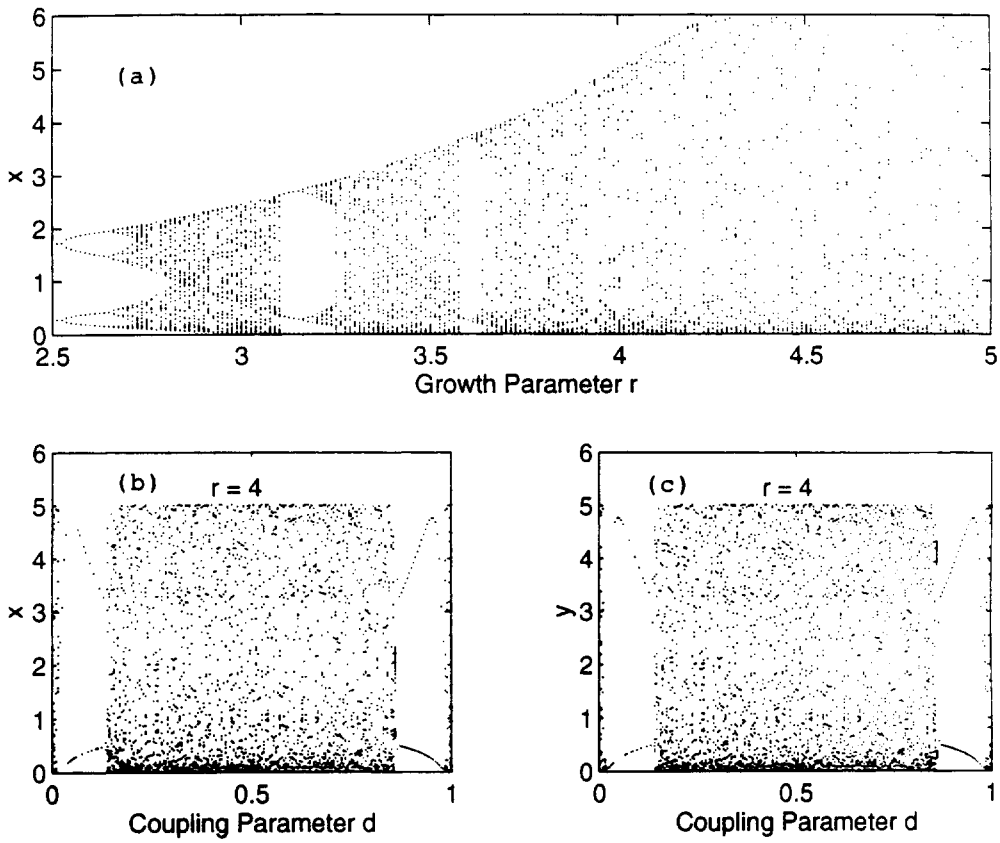

Fig. 1. (a) Bifurcation diagram of the exponential map plotted against the growth parameter r. For many values of r say, $r = 4$, the map is chaotic. By coupling two such maps in the form described by Eq. (2), we can obtain periodic behavior for certain ranges of the coupling parameter d as in (b) and (c).

cubic maps. This is because of the inherently different bifurcation behavior of such maps when compared to maps with negative Schwartzian curvature [15].

The salient features of the dynamics in these seven zones are as follows: (1) In agreement with Result 2 and its corollaries, there is a quasi-symmetry about $d = \frac{1}{2}$, i.e., the dynamical behavior when $d = \frac{1}{2} + k$ is very similar to that when $d = \frac{1}{2} - k$, $0 \leq k \leq \frac{1}{2}$. As a result, the dynamics in zones V, VI, and VII are similar, though *not* identical, to those of zones III, II, and I respectively. (2) Zone I is a region of complex dynamics. This mostly chaotic region does have several periodic orbits. Similar behavior is observed in zone VII, the quasi-symmetric equivalent of zone I. (3) Zone II is characterized by periodic behavior. Similarly, its quasi-symmetric equivalent, zone VI, is periodic. (4) Completely chaotic behavior is observed in both zone III and zone V. (5) Zone IV is chaotic but synchronous, i.e., both the populations are identical in size. It should be noted that though Figs. 1(b) and (c) appear symmetric, there are subtle differences between the trajectories on either side of $d = \frac{1}{2}$. For example, as predicted by Corollary 2, for the range $0.03 \lesssim d \lesssim 0.13$ we have *two one-period* solutions, while for the symmetrically placed range $0.87 < d < 0.97$, we have *one two-period* orbit.

The bifurcations marking the transition from one zone to the other *are also quasi-symmetric* about $d = \frac{1}{2}$. For example, the transition from zone 2 to 1 and that from zone 6 to 7 are both marked by a Sacker (Hopf-like) bifurcation, see Fig. 2(d). The bifurcation from zone 2 to 1 is about a one-period orbit; on the

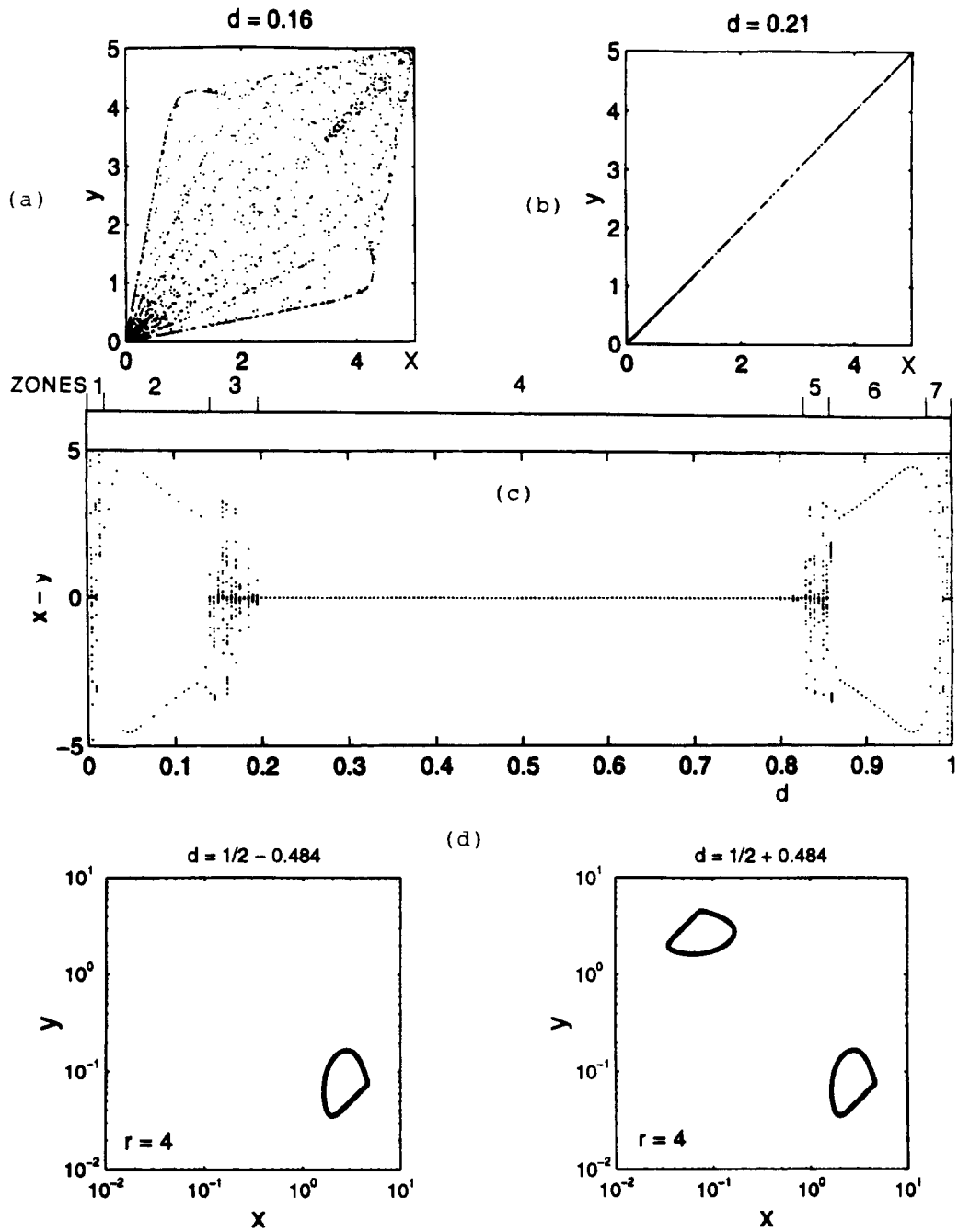

Fig. 2. (a), (b). Plots depicting the diagonal attraction by which orbits emanating from different locations in the xy-plane collapse on to the diagonal. A coupled exponential map with $r = 4$ is used: (a) $d = 0.16$; (b) $d = 0.21$. For some values of d, as in (a), the response is over a region in the line $x = y$. (c) The difference x–y plotted against d. Over a large range of d, the coupled response is synchronous as seen by the null values of the difference x–y. (d) The transitions from zone 2 to zone 1, and from zone 6 to zone 7 are marked by Hopf bifurcations ($r = 4$). The closed loop trajectory on the left is caused by a bifurcation of the one-period orbit in zone 2. The corresponding closed trajectory, caused by a Hopf bifuraction of the two-period orbit in zone 6, is shown on the right. This orbit alternates between the two closed loops. The loops are symmetric about the line $x = y$.

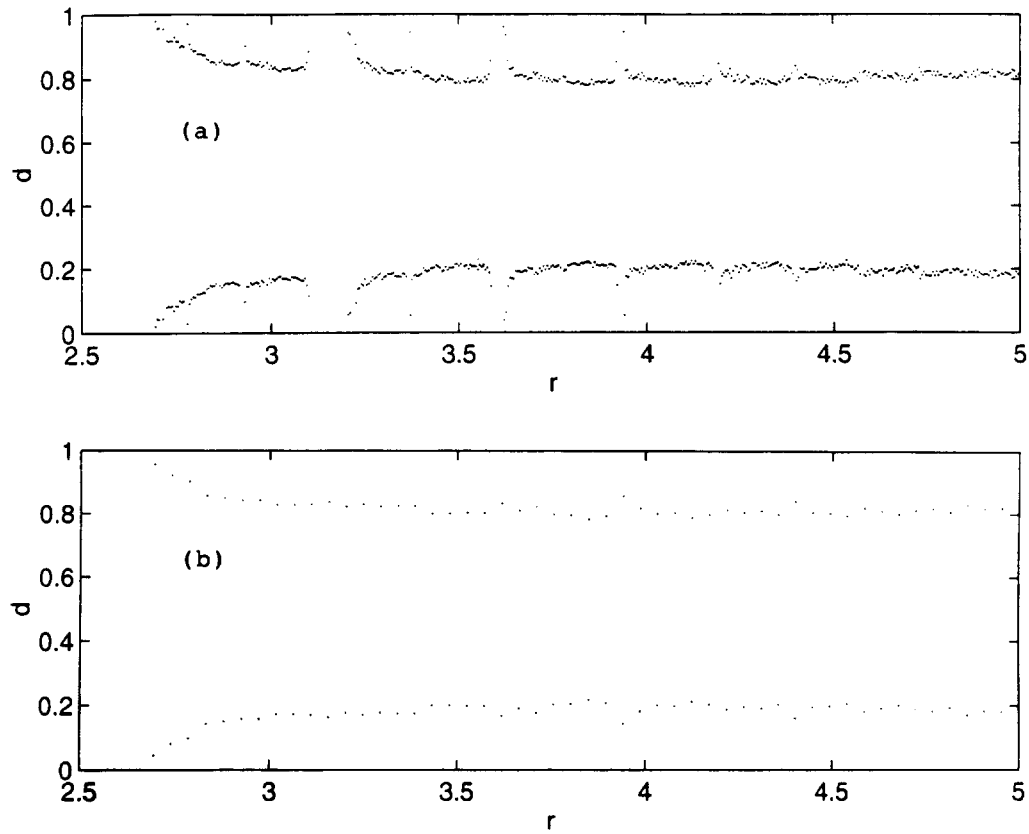

Fig. 3. (a) Range of d for which stable synchronous behavior can be obtained by using linear stability theory. (b) Range of d for which stable synchronous behavior is observed in numerical simulation. The theory and numerical results are in good agreement.

other hand, the bifurcation from zone 6 to 7 is about a two-period orbit. However, the Hopf bifurcation from zone 2 to zone 1, causes the trajectory to follow a single closed curve; on the other hand, the Hopf bifurcation from zone 6 to 7 causes the trajectory to follow *not one but two* closed curves [16]. The transition from zone 2 to 3 and that from zone 6 to 5 are both through a tangent bifurcation leading to an explosive kind of chaos [15]. The bifurcation which delimits the sychronous zone 4 is addressed below. Each zone is thus delineated by bifurcations; the seven-zone dynamics is thus explained by a series of bifurcations that are quasi-symmetric about $d = \frac{1}{2}$.

From the above discussion we can infer that the synchronous behavior in zone IV is stable. It is possible to prove this stability as follows, see also [12,18]. To determine the range of d for which synchronous behavior is stable,we introduce the new variables $u_n = \frac{1}{2}(x_n + y_n)$ and $v_n = \frac{1}{2}(x_n - y_n)$. Eq. (2) can be rewritten as

$$u_{n+1} = \tfrac{1}{2}[f(u_n + v_n) + f(u_n - v_n)], \tag{20}$$

$$v_{n+1} = (2d - 1)[f(u_n + v_n) - f(u_n - v_n)]. \tag{21}$$

Upon linearizing about the point $v_n = 0$, we get

$$u_{n+1} = f(u_n), \tag{22}$$

$$v_{n+1} = (2d - 1)f'(u_n)v_n. \tag{23}$$

Let $\xi_n = \ln|v_n|$ so that the above equation can be reduced to

$$\xi_{n+1} = \xi_n + \ln|2d - 1| + \ln|f'(u_n)| \tag{24}$$

From the above equation the stability threshold can be obtained by averaging over several values of u_n

$$\ln|2d - 1| + \lambda = 0, \tag{25}$$

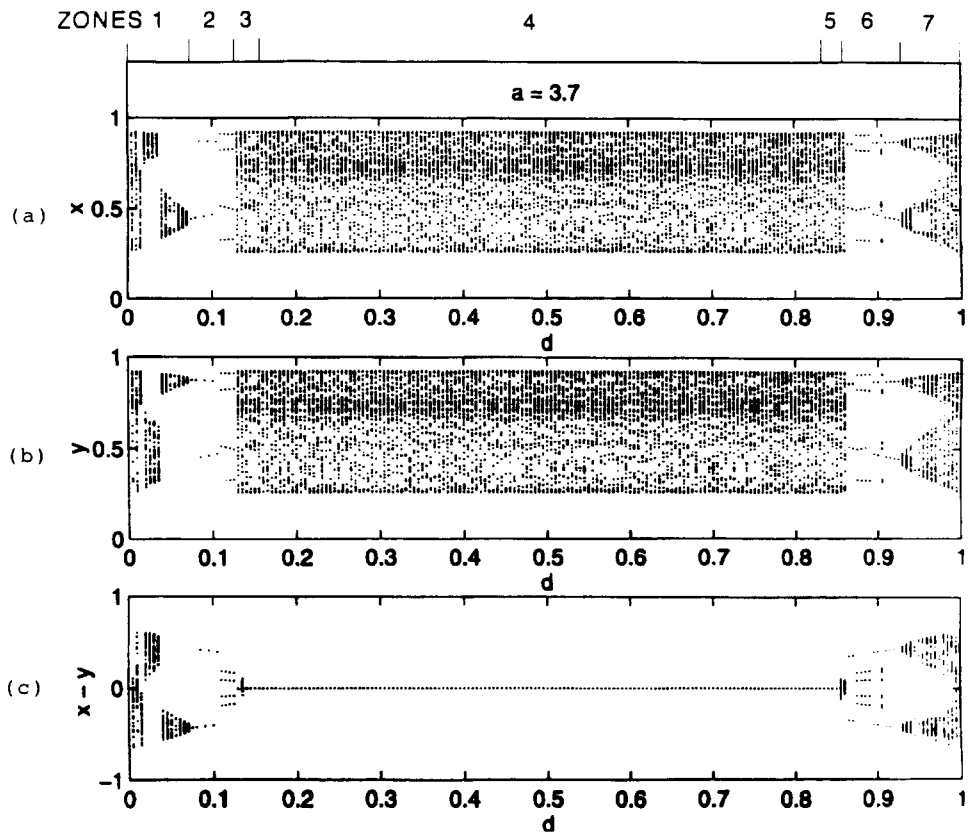

Fig. 4. The seven-zone dynamics for the coupled logistic map. Here the growth rate, a, of the logistic map is 3.7. $(x_0, y_0) = (0.1, 0.75)$.

where λ is the largest Lyapunov exponent. The above equation outlines the two boundaries between which synchronous dynamics is stable. These two boundaries are plotted in Fig. 3(a).

We next compare this theory with numerical results. For a given value of the growth parameter r in the coupled exponential map $(f(x) = x\exp(r(1-x)))$, we obtain the range of d for which synchronous dynamics is observed. To obtain this range we vary d from zero to unity and for each value of d we simulate the dynamics up to 100 000 iterations and check if synchronous dynamics is observed within a numerical accuracy of 10^{-5}. The resulting range of stable synchronous dynamics, plotted in Fig. 3(b), is in good agreement with the corresponding analytical result plotted in Fig. 3(a).

A more detailed description of the seven-zone dynamics can be found in [16]. Here, our focus is on the universal properties of the coupled nonlinear system. And naturally, the first question that arises is whether this seven-zone dynamics is universal. Our numerical simulations demonstrate that this seven-zone dynamics is present in the case of coupled logistic maps as well $(f(x) = ax(1-x)$ in Eq. (2)). When $a = 3.7$, the uncoupled single logistic map is chaotic [10]. The coupled dynamics is plotted in Fig. 4. Again the same seven-zone dynamics is produced; though some finer details of the dynamics of the coupled map may vary with both the initial conditions and the growth parameter a, the general behavior appears to be preserved. This indicates that this seven-zone dynamics may very well be universal for coupled maps wherein each map has negative Schwartzian curvature.

We now return to the coupled exponential map. The pronounced synchronicity or diagonal attraction is striking. Further, there is also a significant range of

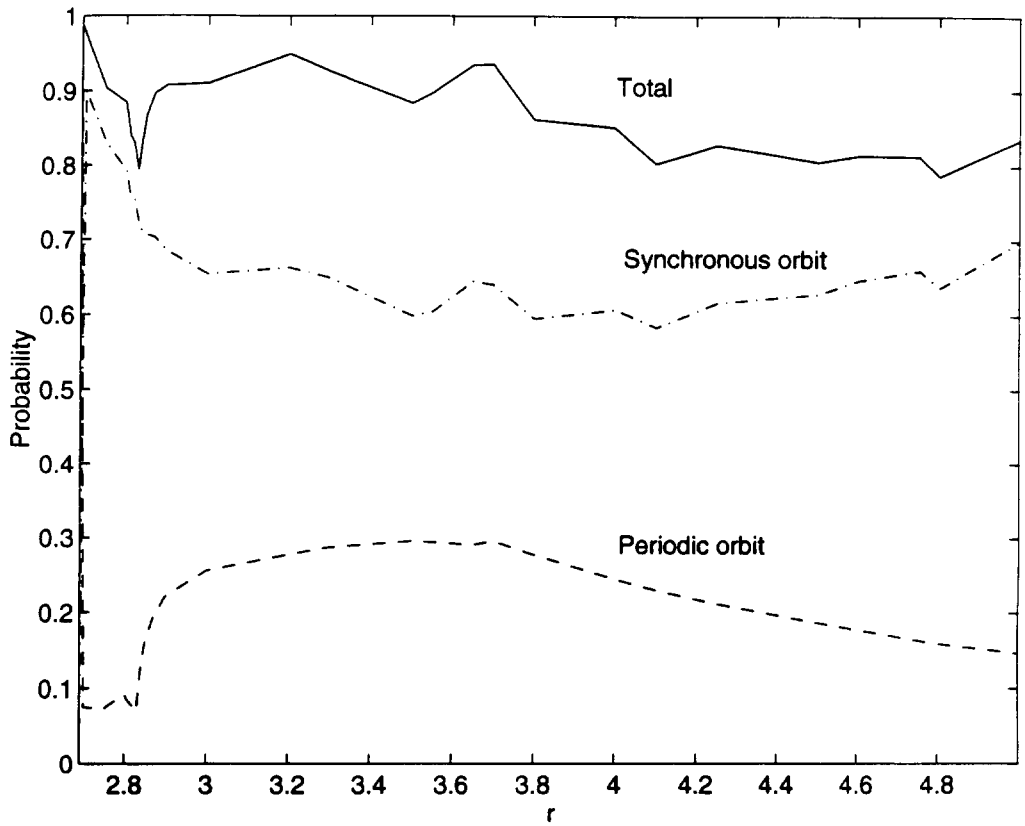

Fig. 5. The probability of obtaining (i) periodic behavior (dashed lines), (ii) synchronous behavior (dashed dot) and (iii) their total, plotted against r. The probability of finding either periodicity or synchronicity is always more than 0.8 for the coupled exponential map.

d over which the dynamical behavior is periodic and one may wonder, given a random coupling (a value of d chosen randomly between 0 and 1), what is the probability of finding periodic or synchronous trajectories. The probability of periodicity, synchronicity, and their total are plotted in Fig. 5 for cases where the underlying single map is chaotic. For every value of $\hat{r}$ chosen, the probabilities are obtained by investigating the orbits for 5000 values of d ranging from zero to unity. The number of periodic orbits produced divided by 5000 yields the probability of periodic orbits and so on. This procedure is repeated over three initial conditions to obtain an average probability. Because the computational time is high we use only a few different initial conditions. Further, the kinks in the probability of synchronicity are related to the chaotic nature of the trajectories and hence difficult to remove. That the probability of finding either a periodic orbit or a synchronous orbit is more than 0.8 indicates that from a probabilistic standpoint, the random coupling of two such chaotic units will most likely result in either a quasi- or a complete stabilization.

It may therefore be appropriate to *posit a hypothesis that highly nonlinear systems which are chaotic can be stabilized by coupling and that it may be because of the coupling of nonlinear systems in real life that the physical world appears orderly.*

Results 2 and 5 outline a set of quasi-symmetry properties. These results indicate that the behavior of the system is somewhat symmetric about $d = \frac{1}{2}$, i.e., if for $d = \frac{1}{2} - d_0$ ($d_0 < \frac{1}{2}$) the dynamics is say periodic, then periodic dynamics will be observed if $d = \frac{1}{2} + d_0$

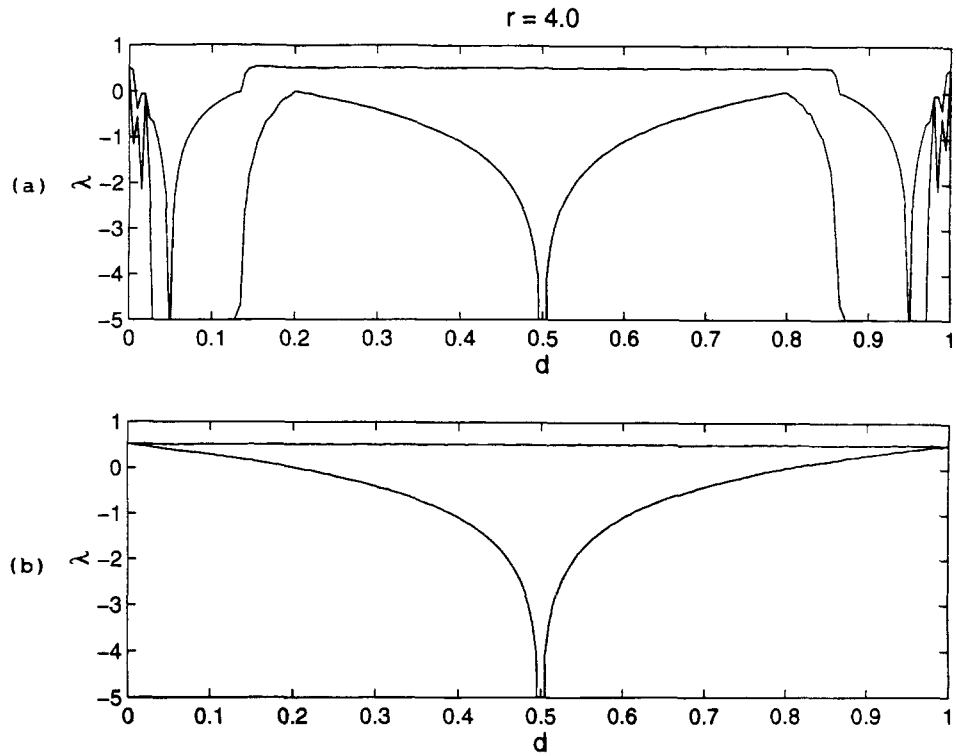

Fig. 6. The spectrum of Lyapunov exponents for different initial conditions (ICs). (a) The ICs do not fall on the diagonal ($x_0 \neq y_0$). There are ranges of d for which both exponents are negative which indicates that the behavior in those ranges is non-chaotic. (b) The ICs fall on the diagonal ($x_0 = y_0$). At least one exponent is positive indicating that the diagonal is chaotic. For both sets of ICs, the exponents are symmetric about $d = \frac{1}{2}$.

given the same initial conditions. Similarly, if for $d = \frac{1}{2} - d_0$ ($d_0 < \frac{1}{2}$) the behavior is chaotic, then chaotic behavior will be observed if $d = \frac{1}{2} + d_0$ given the same initial conditions.

We next analyze the orbits using Lyapunov exponents [1,17]. In Fig. 6, both the Lyapunov exponents of the coupled exponential map ($f(x) = x\exp(r(1-x))$) are plotted against d for two sets of initial conditions. Fig. 6(a) shows the Lyapunov exponents when the initial conditions do not fall on the diagonal ($x_0 \neq y_0$). In Fig. 6(b), the initial conditions fall on the diagonal ($x_0 = y_0$) and as per Result 3, the dynamics is confined to the diagonal. Thus, the dynamics in both these cases is different: in one case the dynamics is not necessarily confined to the diagonal while in the other it is confined to the diagonal. We can readily observe that in each case both the Lyapunov exponents are symmetric about $d = \frac{1}{2}$. However, the dynamical behavior is not truly symmetric, because as demonstrated in Corollary 3, the periodicity of the orbits, for example, may be different.

Further evidence of stability engendered by coupling is shown in Fig. 6(a). When uncoupled ($d = 1$), the two one-dimensional maps are chaotic as seen by their positive Lyapunov exponents. But for certain ranges of d, both the Lyapunov exponents are seen to be negative in Fig. 6(a), again indicating that coupling can lead to stable coupled behavior. These negative exponents describe the evolution of the periodic orbits observed in Fig. 1.

For the case of coupled tent maps Keller et al. [7] have shown that stable two-period trajectories can be obtained by a suitable coupling of two tent maps that are chaotic but whose trajectories in isolation are sufficiently close to two-period motions. We have, on the other hand, demonstrated that periodic trajectories can

be obtained by coupling chaotic exponential maps, whose trajectories in isolation are (in the sense of Lyapunov numbers) far away from periodic behavior.

4. Conclusions

In this paper we have presented several global properties of coupled maps. Though simple to analytically prove, they appear to have gone largely unnoticed in the literature. The results point to a quasi-symmetry about the coupling parameter value $d = \frac{1}{2}$, the time reponse of systems with $d = \frac{1}{2} + d_0$ and $d = \frac{1}{2} - d_0$ being similar *though subtly different*. A similar quasi-symmetry applies to the Lyapunov exponents.

In addition to these analytical results, our numerical simulations show that coupling may enforce either periodic behavior or synchronized (but chaotic) behavior on the dynamics of the coupled map. Thus coupling two systems which in isolation behave chaotically appears to enhance the probability of orderly behavior of the coupled system. We see that the coupled dynamics might be classified, in general, into seven zones. Our investigations suggest that this seven-zone dynamics may also be a global property for it appears to be independent of the functional form of the map, provided it has negative Schwartzian curvature.

References

[1] G. Bennetin, L. Galgani and J.M. Strelcyn, The Lyapunov characteristic exponents for a smooth dynamical systems and for hamiltonian systems; a method for computing all of them. Part 2: Numerical application, Meccanica 15 (1980) 21.

[2] R.A. Chowdhury and K. Chowdhury, Bifurcations in a coupled logistic map, Int. J. Theor. Phys. 30 (1991) 97.

[3] K.M. Cuomo and A.V. Oppenheim, Circuit implementation of synchronized chaos with application to communications, Phys. Rev. Lett. 71 (1993) 65.

[4] A. Engel, P. Konig, A. Kreiter, T. Schillen and W. Singer, Temporal coding in the visual cortex: New vistas on integration in the nervous system, Trends Neurosci. 15 (1992) 218.

[5] H. Fujisaka and T. Yamada, Stability theory of synchronized motion in coupled-oscillator systems, Progr. Theor. Phys. 69 (1983) 32.

[6] M. Gyllenberg, G. Soderbacka and S. Ericsson, Does migration stabilize local population dynamics? Analysis of a discrete metapopulation model, Math. Biosci. 118 (1992) 25.

[7] G. Keller, M. Kunzle and T. Nowicki, Some phase transitions in coupled map lattices, Physica D 59 (1992) 39.

[8] A.K. Kreiter and W. Singer, Oscillatory neuronal responses in the visual cortex of the awake monkey, Eur. J. Neurosci. 4 (1992) 369.

[9] M.S. Livingston, Visually-evoked oscillations in money striate cortex, Soc. Neurosci. Abstr. 17 (1991) 73.3.

[10] R.M. May, Simple mathematical models with very complicated dynamics, Nature 261 (1976) 459.

[11] L. Pecora and T. Carroll, Synchronization in chaotic systems, Phys. Rev. Lett. 64 (1990) 821.

[12] P. Pikovsky and A.S. Grassberger, Symmetry breaking bifurcation for coupled attractors, J. Phys. A 24 (1991) 4587.

[13] W.E. Ricker, Stock and recruitment, J. Fish. Res. Board. Canada 11 (1954) 559.

[14] H.G. Schuster, S. Martin and W. Martienssen, New method for determining the largest Lyapunov exponent of simple nonlinear systems, Phys. Rev. A 33 (1986) 3347.

[15] F.E. Udwadia and R.S. Guttalu, Chaotic dynamics of a piecewise cubic map, Phys. Rev. A 40 (1989) 4032.

[16] F.E. Udwadia and N. Raju, Dynamics of coupled nonlinear maps and its application to ecological modeling, Appl. Math. Comput. 82 (1997) 137.

[17] H. von Bremen, F.E. Udwadia and W. Proskurowski, An efficient qr based method for the computation of Lyapunov exponents, Physica D 101 (1997) 1.

[18] T. Yamada and H. Fujisaka, Stability theory of synchronized motion in coupled-oscillator systems. II – the mapping approach, Progr. Theor. Phys. 70 (1983) 1240.